



# Decision Support for Removing Fractured Endodontic Instruments: A Patient-Specific Approach

Raphaël Richert, Jean-Christophe Farges, Cyril Villat, Sebastien Valette,  
Philippe Boisse, Maxime Ducret

## ► To cite this version:

Raphaël Richert, Jean-Christophe Farges, Cyril Villat, Sebastien Valette, Philippe Boisse, et al..  
Decision Support for Removing Fractured Endodontic Instruments: A Patient-Specific Approach.  
Applied Sciences, 2021, 11 (6), pp.2602. 10.3390/app11062602 . hal-03370481

**HAL Id: hal-03370481**

**<https://hal.science/hal-03370481>**

Submitted on 12 Oct 2021

**HAL** is a multi-disciplinary open access archive for the deposit and dissemination of scientific research documents, whether they are published or not. The documents may come from teaching and research institutions in France or abroad, or from public or private research centers.

L'archive ouverte pluridisciplinaire **HAL**, est destinée au dépôt et à la diffusion de documents scientifiques de niveau recherche, publiés ou non, émanant des établissements d'enseignement et de recherche français ou étrangers, des laboratoires publics ou privés.

# Decision support in removing fractured endodontic instruments: a patient-specific approach

Raphaël Richert<sup>1,2</sup>, Jean-Christophe Farges<sup>1,3</sup>, Cyril Villat<sup>1,4</sup>, Sébastien Valette<sup>5</sup>, Philippe Boisse<sup>2</sup>,  
Maxime Ducret<sup>1,3</sup>

1 :Hospices Civils de Lyon, PAM d'Odontologie, Lyon, France;

2 : Laboratoire de Mécanique des Contacts et Structures, UMR 5259 CNRS/INSA, Villeurbanne, France;

3 :Laboratoire de Biologie tissulaire et Ingénierie thérapeutique, UMR5305 CNRS/UCBL, Lyon, France;

4 :Laboratoire des Multimatériaux et Interfaces, UMR CNRS 5615/UCBL, Lyon, France;

5 :Centre de Recherche en Acquisition et Traitement de l'Image pour la Santé, CNRS UMR 5220/INSERM U1206/INSA, Villeurbanne, France

**Abstract:** **Aim:** instrumental fracture is a common endodontic complication that is treated by surgical or non-surgical removal approaches. However, no tool exists to help the clinician to choose between available strategies, and decision-making is mostly based on clinical judgment. Digital solutions, such as Finite Element Analysis (FEA) and Virtual Treatment Planning (VTP), were recently proposed in maxillofacial surgery to help in this regard. The aim of the present paper is to present a digital tool to choose between non-surgical and surgical strategies in a clinical situation of fractured instrument (FI). **Material and methods:** patient tooth data were recorded using cone beam computed tomography (CBCT). VTP was conducted using an application suited for medical images to segment and plan the procedure. FEA has been carried out using the Abaqus software according to published material properties. Five models have been created: the initial state of the patient, two non-surgical removal strategies using a low or high root canal enlargement, and two surgical removal strategies using a 3- or 6-mm apicoectomy. **Results:** Results of the VTP found a risk of perforation for the non-surgical strategies and a sinus proximity for surgical ones. FEA identified the lowest mechanical risk for the 3-mm apicoectomy strategy. A 3-mm apicoectomy approach was finally chosen and performed. **Conclusion:** this digital approach could offer a decision tool for the instrument removal by planning the treatment and predicting the mechanical impact of each strategy.

**Keywords:** Finite Element Analysis; Virtual treatment planning; Endodontics; Apicoectomy; Instrument removal; Decision-making

## Introduction

The fracture of an endodontic instrument within the root canal is a common complication of endodontic treatments (0.25 to 7.41%), most fractures occurring in the apical third of the root<sup>1,2</sup>. This fracture can affect tooth prognosis and several instrument removal strategies have been reported to complete the endodontic treatment<sup>3,4</sup>. A non-surgical strategy was proposed using ultrasonic tips to loosen the fractured instrument, but this procedure can lead to canal over enlargement or root perforation<sup>5,6</sup>. A surgical strategy was also reported to remove the instrument after performing an apicoectomy<sup>7</sup>, but it induces a reduction of the crown-to-root ratio<sup>8,9</sup>. Both strategies thus mechanically impact the tooth and the success of the endodontic retreatment<sup>10,11</sup>. Nowadays, there is no tool to guide the clinician in choosing between these strategies, and decision- making is mostly based on clinical judgment instead of scientific evidence<sup>3</sup>.

Digital approaches have been used for many years; for instance, Virtual Treatment Planning (VTP) has been used to improve the reconstruction accuracy and outcome in the maxillofacial field<sup>12,13</sup>. Similarly, patient-specific Finite Element Analysis (FEA) was reported to provide better predictions on bone fracture than what experienced clinicians predict in orthopedic practice<sup>14</sup>. In endodontics, FEA has been used to evaluate the influence of the instrument position and the resection length on the root stress distribution<sup>15-17</sup>. However, these studies used standard anatomic dimensions to create finite element (FE) models while the success rate mainly depends on patient-specific parameters such as bone loss and canal anatomy<sup>6,9,18</sup>. A recent study proposed to combine VTP and FEA for computer-aided decision-making, with the aim to predict the mechanical behavior of different maxillofacial surgeries and choose the most adapted solution for the patient<sup>19</sup>. Herein, we report a case of an endodontic instrument fracture and the application of a digital approach combining VTP and FEA to help decide between surgical and non-surgical strategies for its removal.

## Case report

### *Case presentation*

A 26-year-old female patient was addressed to the department of endodontics of the Lyon University Hospital with a instrument fractured (FI) in the root canal of her right second maxillary premolar. The 8 mm-long instrument was fractured during an initial endodontic treatment of irreversible pulpitis, one week earlier. The patient reported no pain since the fracture occurred. Clinical examination of the premolar crown indicated presence of four dental walls and a recent temporary restoration on the occlusal face. The tooth presented no cold response, no percussion or palpation tenderness, and physiological mobility. The intraoral periapical radiograph confirmed the transfixated position of the instrument, close to the sinus, and the absence of periapical radiolucency or local swelling of the sinus membrane. The patient tooth was scanned before any intervention to evaluate the instrument position using cone beam computed tomography (CBCT; Planmeca ProMax 3D, Helsinki, Finland) operating at 120 kV, 100 mAs, with a slice thickness of 0.75 mm. The data were recorded under the Digital Imaging and Communication in Medicine (DICOM) format and analyzed. Two non-surgical and surgical strategies emerged from the discussions of the healthcare team, but no consensus was reached on the treatment that could ensure the best outcome. A digital approach, combining VTP and FEA <sup>19</sup>, was then implemented to visualize the planned treatment and predict the mechanical impact of the two removal strategies (Fig 1).

### *Virtual treatment planning*

The different anatomical structures were segmented using DESK, an application suited for medical images <sup>20</sup>. The semi-automatic segmentation is based on the attribution of pixel labels, “seeds”, inside each anatomical structure and a growing region algorithm. Four labels were generated according to the structures of “air”, “tooth”, “bone”, and “intra-root canal material”

to produce a multi-label 3D image. This initial 3D image was then modified to simulate the procedures of the different removal strategies.

Five clinical situations were considered by the healthcare team: the initial state of the patient, two simulated non-surgical removal strategies using a low or high root canal enlargement, and two simulated surgical removal strategies using a 3- or 6-mm apicoectomy.

An ultrasonic tip (ET25; Satelec, Bordeaux, France) was modelled by a conical cylinder 0.5 mm in diameter and a 4% taper, and recorded under STL format for VTP of non-surgical approaches. The surface of the tip was then superimposed along one third of the instrument either on the distal side of the instrument to simulate a low root canal enlargement, or on the distal and vestibular sides of the instrument to simulate a high root canal enlargement. VTP of surgical approaches was conducted with a 3- or 6-mm root shortening (Fig 2A).

The different virtual removal strategies were analyzed on the 3D modified image. The latter offers the operator the possibility to add or suppress masks of bone, ultrasonic tip or instrument to plan his procedure. For non-surgical strategies, the high enlargement was associated to a long perforation. VTP of surgical strategies were also informative on the reduction of the crown-root ratio (Fig. 2A). The 3D modified image could also be used to simulate the clinical point of view of the dental practitioner. For non-surgical strategies, the location of the instrument and the long perforation were difficult to perceive on the simulated clinical view. The clinical view of surgical strategies also enables to plan the possible access ways that avoid sinus perforation (Fig. 2B).

#### *Finite element modelling and mechanical analysis*

Modified 3D images were then meshed with tetrahedral elements using the Computational Geometry Algorithms Library (CGAL) meshing library <sup>20</sup> imported in the FEA software Abaqus (Dassault Systèmes, Vélizy-Villacoublay, France; Fig. 3). The periodontal ligament

could not be detected on the DICOM and was simulated around the root surface with a thickness of 250  $\mu\text{m}$  <sup>21</sup>. The attributed material properties (Table 1) were referenced from the literature <sup>21–23</sup>. All materials were supposed homogeneous, linear and elastic, and there was a perfect bonding between each component <sup>16</sup>. The occlusal faces were not modelled due to x-ray artefacts. A vertical load of 150 N was distributed on the top surface of the root and the nodes of the base, and lateral faces of the bone were constrained to prevent displacement <sup>16</sup>. A static explicit analysis was conducted to calculate principal strains and Von Mises stresses for all FE models. The mechanical behavior of the tooth was evaluated by comparing the Von Mises stress distribution and the maximal Von Mises stress (fracture criterion) <sup>24</sup> between all FE models. Each FE model was verified using a convergence test <sup>25</sup> and the Zhu-Zienkiewicz error estimator <sup>26</sup> (Table 2).

The apicoectomy models presented a lower fracture criterion than enlargement models and the model of the initial state of the patient. The 3-mm apicoectomy model presented the lowest stress value, whereas the high enlargement model presented the highest fracture criterion of all models (Table 3). Regarding stress distribution, high values around the instrument were found in the initial model; high values around the perforation were found in the enlargement models; and high values on the resected surface were found in apicoectomy models (Fig 3). The error indicator was considered as acceptable <sup>27,28</sup> for all models, indicating that this method provides valuable models for FEA.

#### *Management of the fractured instrument*

After having informed the patient about the possible treatments, a 3-mm apicoectomy strategy was decided in accordance with her. First, the orthograde root canal treatment up to the fractured instrument and the tooth restoration were completed. One week later, the micro apical surgery was conducted following a 3-mm apicoectomy. The root end and the instrument were removed as a single entity to avoid risk of instrument projection into the sinus <sup>29</sup> and the root end was

inspected under high magnification. The root canal was treated in a minimally invasive way using only a 3-mm ultrasonic retro-tip and the quality of the obturation was controlled on a periapical radiograph. The patient returned to her referent practitioner for the prosthetic rehabilitation, and the tooth remained asymptomatic at six weeks follow-up. The periapical radiograph at six months showed bone healing and absence of periapical radiolucency (Fig 4).

## **Discussion**

This is the first work to report the use of digital technologies as decision support between non-surgical and surgical strategies of removal of a fractured endodontic instrument. In the present case, the digital approach allowed to visualize and anticipate the patient-specific root and sinus perforation, and to predict the mechanical impact of four removal strategies.

Studies reported that clinicians have difficulties to orient themselves in space from CBCT slices during their surgical procedure <sup>30</sup>. Herein, VTP was used to simulate the procedures using a multi-label 3D image and to predict the iatrogenicity of the procedure. Increased risks of perforation and complications were reported for removal of apically fractured instruments <sup>31</sup>. The 3D image enabled to precisely evaluate the presence of perforation and the position of the sinus using the clinical view. It is of note that the use of a printed guide increases the accuracy and reduces the risk of sinus perforation during endodontic microsurgery <sup>32</sup>. However, this was not used in the case presented herein owing to the risk of instrument projection into the sinus.

In the current case, surgical strategies present a more favorable stress distribution than non-surgical ones, which supports herein the apicoectomy. This conclusion was also recommended by a previous narrative review promoting a surgical approach in cases of a separated instrument in the apical part of the root <sup>3</sup>. Regarding the resection level, a 3-mm apicoectomy presents lower stress values than a 6-mm apicoectomy, which is in accordance with previous FEA



studies <sup>9,33</sup>. However, if a short resection is not sufficient to remove the instrument, increasing the resection level appears herein mechanically more acceptable than non-surgical strategies.

Despite the apparent value of the presented strategy, several limitations are to be highlighted. The main one is that the accuracy of CBCT is questionable in the occlusal part due to artifacts, whereas it is known that occlusal morphology influences the stress distribution in FEA <sup>34,35</sup>. Recent technologies such as micro CBCT <sup>36</sup> and the use of an intraoral scanner avoiding x-ray artefacts <sup>37</sup> could improve future simulations. FEA results should also be carefully interpreted due to the technical impossibility to identify patient-specific parameters such as force intensity <sup>38</sup> or for ligament modeling <sup>39</sup>. Both VTP and FEA also required supplementary software and operator skills, which makes their use in routine clinical practice complex. The development of an intuitive software, marked as a medical device, will be necessary in the future to allow a wide dissemination of this technique among dental practitioners.

## **Conclusion**

The case presented in this report illustrates some benefits of computer-aided solutions for decision-making in the removal of fractured endodontic instruments, by planning the treatment and predicting the mechanical impact induced by non-surgical and surgical strategies. Further investigations are required to confirm the relevance of this digital approach and improve the current software for routine clinical practice.

## Acknowledgements

This study did not receive any specific grant from funding agencies in the public, commercial, or not-for-profit sectors.

## References

1. Iqbal, MK, Kohli MR. & Kim JS. A Retrospective Clinical Study of Incidence of Root Canal Instrument Separation in an Endodontics Graduate Program: A PennEndo Database Study. *J Endod* 2006;32:1048–1052.
2. Tzanetakakis GN, Kontakiotis EG, Maurikou DV, Marzelou MP. Prevalence and Management of Instrument Fracture in the Postgraduate Endodontic Program at the Dental School of Athens: A Five-year Retrospective Clinical Study. *J Endod* 2008;34:675–678.
3. Madarati AA, Hunter MJ, Dummer PMH. Management of Intracanal Separated Instruments. *J Endod* 2013;39:569–581.
4. McGuigan MB, Louca C, Duncan, HF. Clinical decision-making after endodontic instrument fracture. *Br Dent J* 2013;214:395–400.
5. Panitvisai P, Parunnit P, Sathorn C, Messer HH. Impact of a Retained Instrument on Treatment Outcome: A Systematic Review and Meta-analysis. *J Endod* 2010;36:775–780.
6. Suter B, Lussi A, Sequeira P. Probability of removing fractured instruments from root canals. *Int Endod J* 2005;38:112–123.
7. Setzer FC, Shah SB, Kohli MR, Karabucak B, Kim S. Outcome of Endodontic Surgery: A Meta-analysis of the Literature ;Part 1: Comparison of Traditional Root-end Surgery and Endodontic Microsurgery. *J Endod* 2010;36:1757–1765.
8. von Arx T, Jensen S, Bornstein M. Changes of Root Length and Root-to-Crown Ratio after Apical Surgery: An Analysis by Using Cone-beam Computed Tomography. *J Endod* 2015;41:1424–1429.

9. Jang Y, Hong HT, Roh BD, Chun HJ. Influence of apical root resection on the biomechanical response of a single-rooted tooth: a 3-dimensional finite element analysis. *J Endod* 2014;40:1489–1493.
10. Schestatsky R, Dartora G, Felberg R, Spazzin AO, Sarkis-Onofre R, Bacchi A, Pereira GKR. Do endodontic retreatment techniques influence the fracture strength of endodontically treated teeth? A systematic review and meta-analysis. *J Mech Behav Biomed Mater* 2019;90:306–312.
11. Soares CJ, Rodrigues MP, Faria-E-Silva AL, Santos-Filho PCF, Veríssimo C, Kim HC, Versluis A. How biomechanics can affect the endodontic treated teeth and their restorative procedures? *Braz Oral Res* 2018;32:169–183.
12. Rodby KA, Turin S, Jacobs RJ, Cruz JF, Hassid VJ, Kolokythas A, Antony AK. Advances in oncologic head and neck reconstruction: Systematic review and future considerations of virtual surgical planning and computer aided design/computer aided modeling. *J Plast Reconstr Aesthetic Surg* 2014;67:1171–1185.
13. Tang NSJ, Ahmadi I, Ramakrishnan A. Virtual surgical planning in fibula free flap head and neck reconstruction: A systematic review and meta-analysis. *J Plast Reconstr Aesthetic Surg* 2019;72:1465–1477.
14. Eggermont F, van der Wal G, Westhoff P, Laar A, de Jong M, Rozema T, Kroon HM, Ayu O, Derikx L, Dijkstra S, Verdonschot N, van der Linden Y, Tanck E. Patient-specific finite element computer models improve fracture risk assessments in cancer patients with femoral bone metastases compared to clinical guidelines. *Bone* 2020;130.
15. Ni N, Ye J, Wang L, Shen S, Han L, Wang Y. Stress distribution in a mandibular premolar after separated nickel-titanium instrument removal and root canal preparation: a three-dimensional finite element analysis. *J Int Med Res* 2019; 47:1555–1564.
16. Kim S, Park SY, Lee Y, Lee CJ, Karabucak B, Kim HC, Kim E. Stress Analyses of Retrograde Cavity Preparation Designs for Surgical Endodontics in the Mesial Root of the Mandibular Molar: A Finite Element Analysis ;Part I. *J Endod* 2019; 45:442–446.
17. Gümrükçü Z, Kurt S, Köse, S. Effect of Root Resection Length and Graft Type Used After Apical Resection: A Finite Element Study. *J Oral Maxillofac Surg* 2019;77.

18. Nevares G, Cunha RS, Zuolo ML, da Silveira Bueno CE. Success Rates for Removing or Bypassing Fractured Instruments: A Prospective Clinical Study. *J Endod* 2012;38:442–444.
19. Beldie L, Walker B, Lu Y, Richmond S, Middleton J. Finite element modelling of maxillofacial surgery and facial expressions—a preliminary study. *Int J Med Robot Comput Assist Surg* 2010;6:422–430.
20. Jacinto H, Kéchichian R, Desvignes M, Prost R, Valette S. A web interface for 3D visualization and interactive segmentation of medical images. *17th Int Conf 3D Web Technol* 2012;17:51–58.
21. Chang YH, Lee H, Lin CL. Early resin luting material damage around a circular fiber post in a root canal treated premolar by using micro-computerized tomographic and finite element sub-modeling analyses. *J Mech Behav Biomed Mater* 2015;51:184–193 (2015).
22. Thompson SA. An overview of nickel – titanium alloys used in dentistry. *Int Endod J* 2000;33:297–310.
23. Hondrum SO. Temporary dental restorative materials for military field use. *Mil Med* 1998;163:381–385.
24. Juloski J, Apicella D, Ferrari M. The effect of ferrule height on stress distribution within a tooth restored with fibre posts and ceramic crown: A finite element analysis. *Dent Mater* 2014;30:1304–1315.
25. Erdemir A, Guess TM, Halloran J, Tadepalli SC, Morrison TM. Considerations for reporting finite element analysis studies in biomechanics. *J Biomech* 2012;45:625–633.
26. Zhu, JZ, Zienkiewicz OC. A posteriori error estimation and three-dimensional automatic mesh generation. *Finite Elem Anal Des* 1997;25:167–184.
27. Fischer A, Eidel B. Convergence and Error Analysis of FE-HMM/FE for Energetically Consistent Micro-Coupling Conditions in Linear Elastic Solids. *Eur J Mech A/Solids* 2019;77.
28. Fischer A, Eidel B. Error analysis for quadtree-type mesh coarsening algorithms adapted to pixelized heterogeneous microstructures. *Comput Mech* 2020;65.
29. Hauman CHJ, Chandler NP, Tong DC. Endodontic implications of the maxillary sinus: A review. *Int Endod J* 2002;35:127–141.

30. Scarfe WC, Levin MD, Gane D, Farman AG. Use of Cone Beam Computed Tomography in Endodontics. *Int J Dent* 2009;634567.
31. Parashos P, Messer HH. Rotary NiTi Instrument Fracture and its Consequences. *J Endod* 2006;32:1031–1043.
32. Giacomino CM, Ray JJ, Wealleans JA. Targeted Endodontic Microsurgery : A Novel Approach to Anatomically Challenging Scenarios Using 3-dimensional – printed Guides and Trephine Burs — A Report of 3 Cases. *J Endod* 2018;44:1–7.
33. Ran SJ, Yang X, Sun Z, Zhang Y, Chen JX, Wang DM, Liu B. Effect of length of apical root resection on the biomechanical response of a maxillary central incisor in various occlusal relationships. *Int Endod J* 2020; 53, 111–121 (2020).
34. Benazzi S, Grosse IR, Gruppioni G, Weber GW, Kullmer O. Comparison of occlusal loading conditions in a lower second premolar using three-dimensional finite element analysis. *Clin Oral Investig* 2014;18:369–375.
35. Murakami N, Wakabayash, N. Finite element contact analysis as a critical technique in dental biomechanics: A review. *J Prosthodont Res* 2014; 58, 92–101 (2014).
36. Acar B, Kamburoğlu K, Tatar I, Arıkan V, Çelik HH, Yüksel S, Özen T. Comparison of micro-computerized tomography and cone-beam computerized tomography in the detection of accessory canals in primary molars. *Imaging Sci Dent* 2015;45:205–211.
37. Rangel FA, Maal TJJ, Bronkhorst EM, Breuning KH, Schols JGJH, Bergé SJ, Kuijpers-Jagtman AM. Accuracy and Reliability of a Novel Method for Fusion of Digital Dental Casts and Cone Beam Computed Tomography Scans. *PLoS One* 2013;8:1–7.
38. Richert R, Farges JC, Tamimi F, Naouar N, Boisse P, Ducret M. Validated Finite Element Models of Premolars: A Scoping Review. *Materials* 2020.13.
39. Papadopoulou K, Hasan I, Keilig L, Reimann S, Eliades T, Jäger A, Deschner J, Bourauel C. Biomechanical time dependency of the periodontal ligament: A combined experimental and numerical approach. *Eur J Orthod* 2013;35:811–818.

40. Ha WN, Nicholson T, Kahler B, Walsh L J. Methodologies for measuring the setting times of mineral trioxide aggregate and Portland cement products used in dentistry. *Acta Biomater Odontol Scand* 2016;2:25–30.

**Table 1** Material properties <sup>21,22,40</sup>.

<b>Material</b>	<b>Young's modulus (GPa)</b>	<b>Poisson's ratio</b>	<b>Reference</b>
Dentine	18.6	0.31	21
Ligament	0.069	0.45	21
Trabecular bone	1.3	0.3	21
Gutta percha	0.069	0.45	21
Root-end filling (modified zinc-oxyde eygenol)	0.1	0.31	23
Instrument (ProTaper Gold <sup>®</sup> )	50	0.26	22

**Table 2** Number of elements, nodes, and error indicator according to the finite element model considered.

Model	Number of elements	Number of nodes	Zhu-Zienkiewicz error indicator	Mean coronal strain
Initial State	202636	29742	9.1 %	$2.4 \cdot 10^{-4}$
Low enlargement	202462	29637	9.2 %	$2.4 \cdot 10^{-4}$
High enlargement	202027	29614	9.3 %	$2.4 \cdot 10^{-4}$
3-mm apicoectomy	201714	29855	8.9 %	$2.4 \cdot 10^{-4}$
6-mm apicoectomy	207250	31126	9.2 %	$3.2 \cdot 10^{-4}$



**Table 3** Patient-specific analysis based on the 3D image and maximal Von Mises stress of the different removal strategies.

	Analysis of the 3D image	High stress location	Fracture criterion
Initial state	No	Around the instrument	444.7 MPa
<b>Removal strategy</b>			
Low enlargement	Apical perforation	Around the perforation	367.3 MPa
High enlargement	Lateral perforation	Around the perforation	546.4 MPa
3-mm apicoectomy	Decrease of the crown- root ratio	Resected apex	109.9 MPa
6-mm apicoectomy	Decrease of the crown- root ratio	Resected apex	138.6 MPa

*Process for a patient-specific therapeutics analysis*

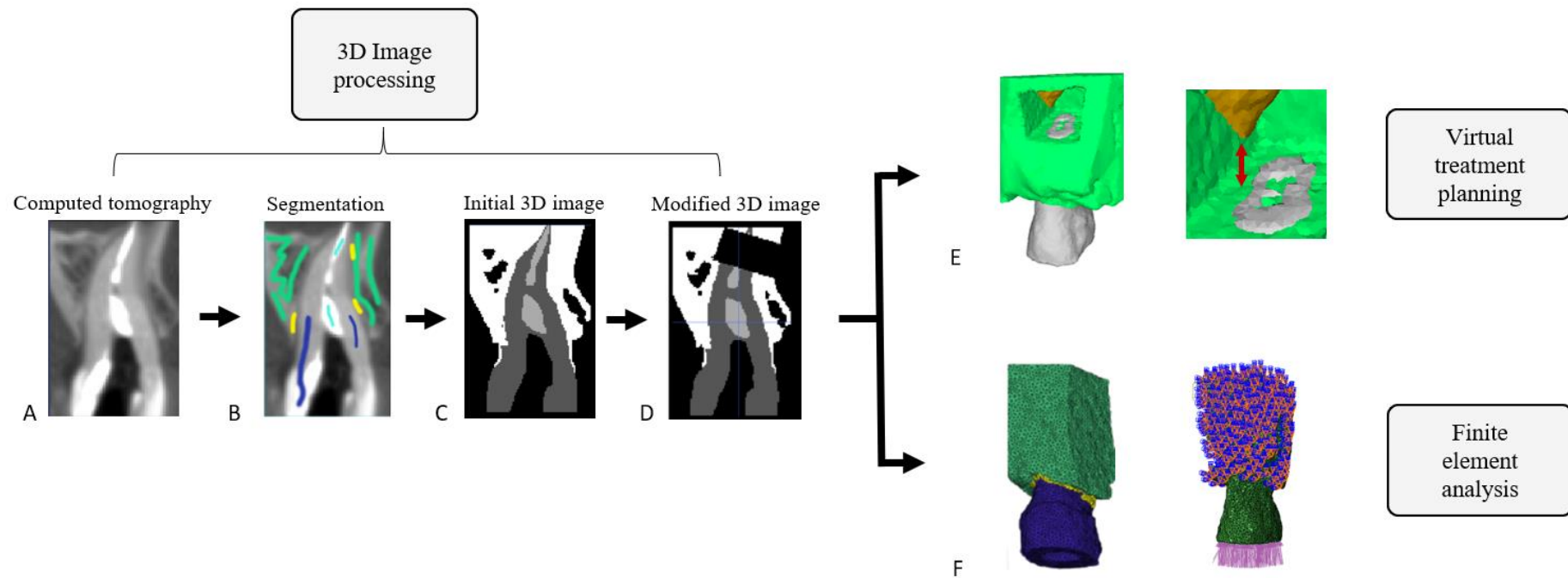


**Fig 1** Process for a patient-specific biomechanical analysis and detailed steps for virtual treatment planning and finite element analysis: (A) axial view of Cone Beam Computed Tomography, (B) attribution of pixel labels, “seeds”, inside each anatomical structure, (C) segmentation based on a growing region algorithm, (D) transformation of the initial 3D image to simulate a 3-mm apicoectomy, (E) analysis of the 3D simulated treatment, and (F) meshing of the 3D transformed image to get a finite element model, and application of boundary conditions.

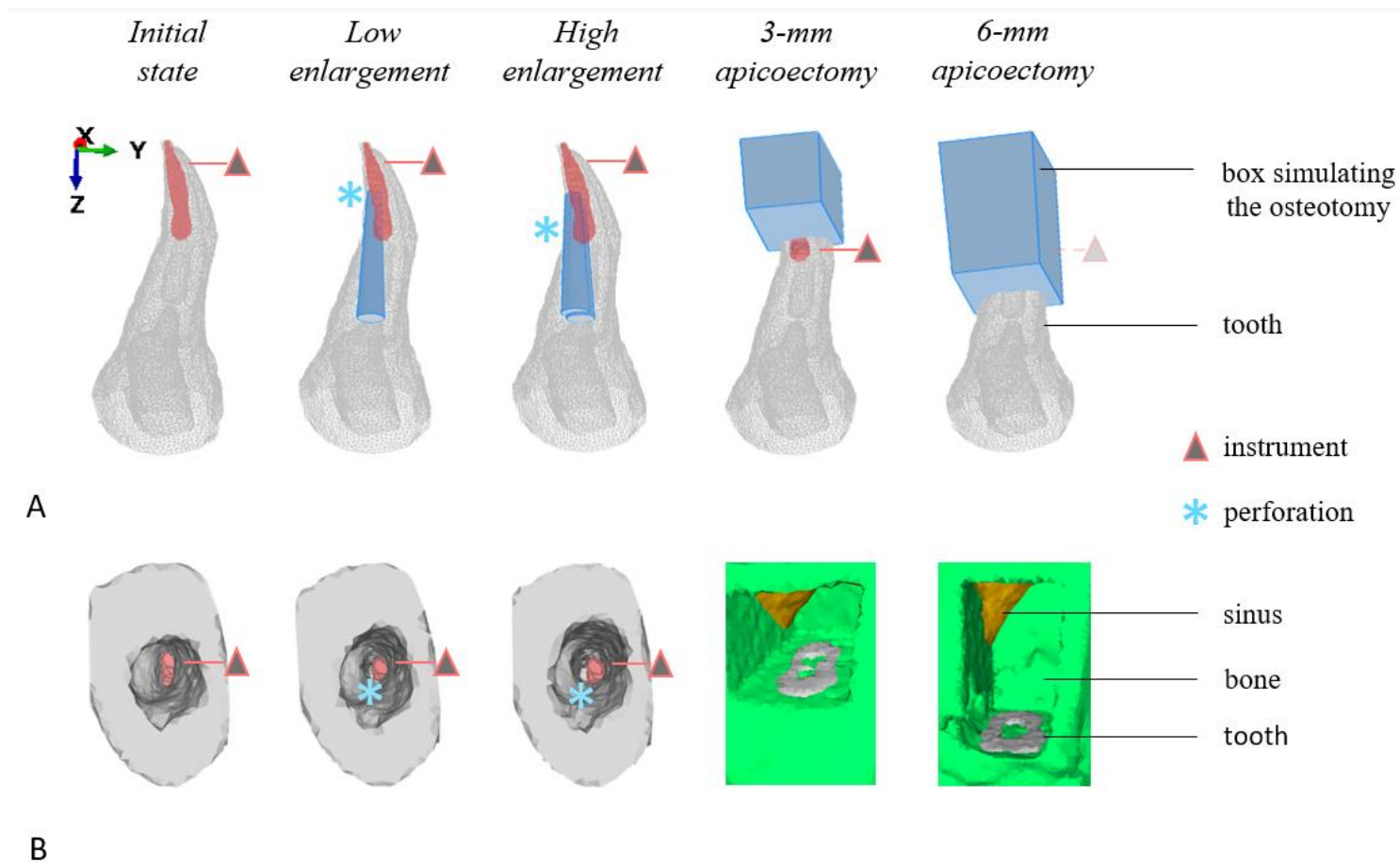


**Fig 2** 3D images for each situation of the virtual treatment planning. (A) Superimposition on the initial 3D image of the surfaces of the ultrasonic tip for enlargement strategies and osteotomy for apicoectomy strategies. (B) simulated clinical views of the initial 3D image and of the modified 3D images for each removal strategy.

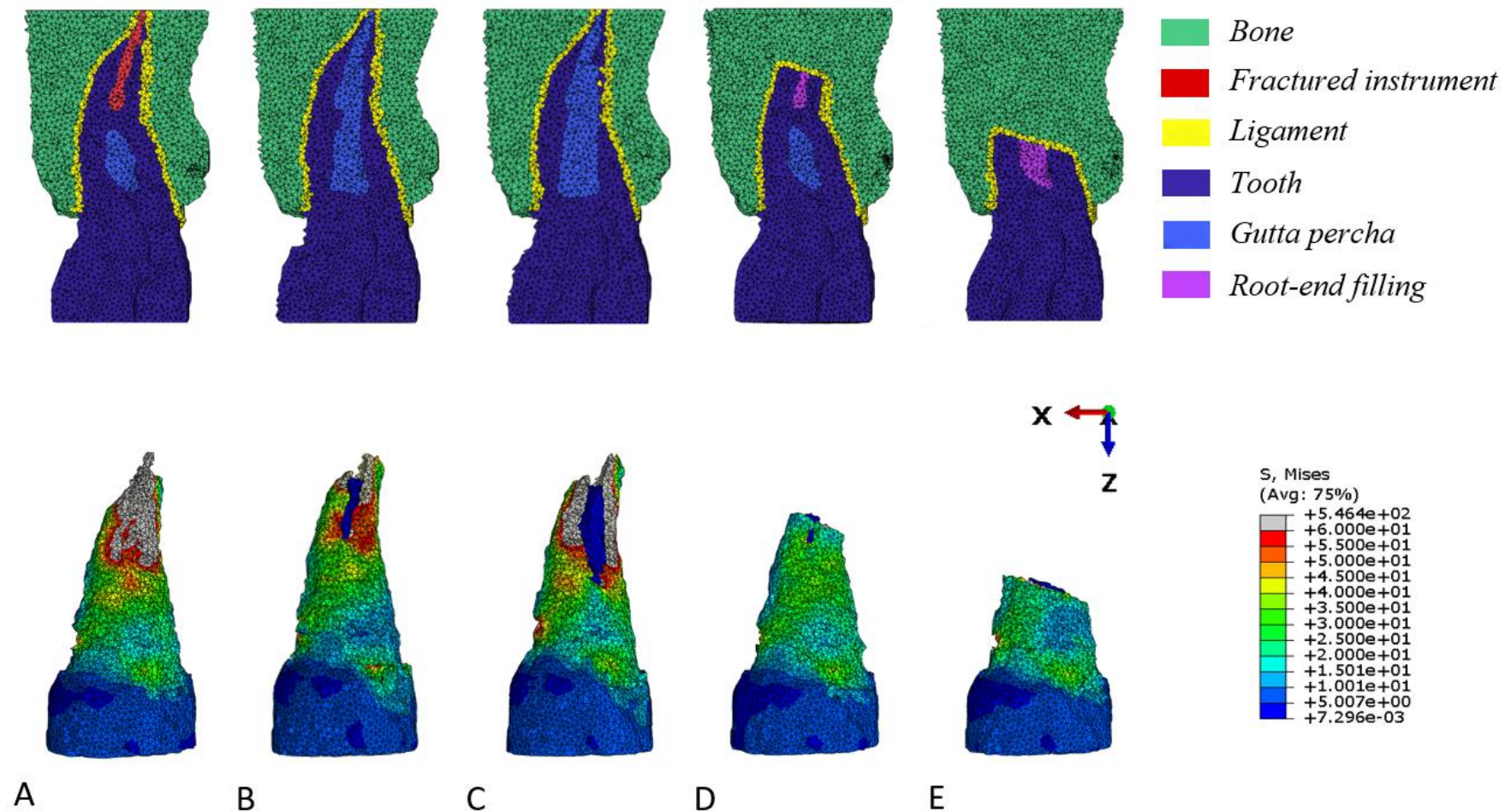


**Fig 3** Cut views for each mesh and buccal views of Von Mises root stress represented by color, from blue (low values) to red (high values), for each finite element model. (A) Initial model representing the initial state, (B) low enlargement model, (C) high enlargement model, (D) 3-mm apicoectomy model, and (E) 6-mm apicoectomy model.



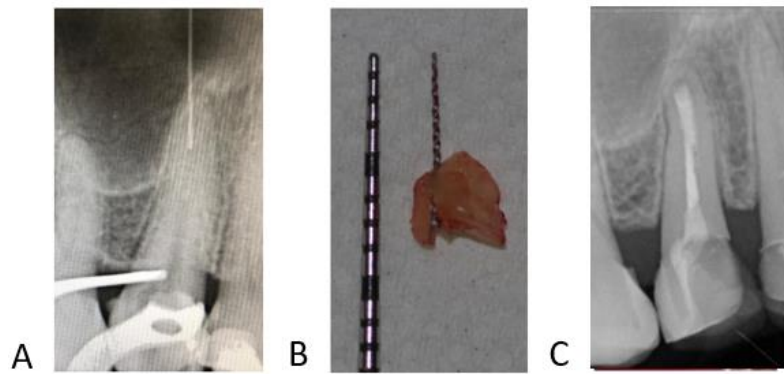


**Fig 4** Micro apical surgery of the maxillary premolar. (A) Initial radiograph after instrument fracture, (B) size of the resected apex and of the removed instrument, and (C) postoperative radiograph at six months.